

PHYSICAL REVIEW B

CONDENSED MATTER

THIRD SERIES, VOLUME 40, NUMBER 17

15 DECEMBER 1989-I

Novel metal-film configuration: Rh on Ag(100)

P. J. Schmitz, W.-Y. Leung, G. W. Graham,* and P. A. Thiel

Department of Chemistry and Ames Laboratory, Iowa State University, Ames, Iowa 50011

(Received 17 April 1989)

We present the results of an investigation of Rh films on Ag(100). The films are studied using Auger-electron spectroscopy, low-energy electron diffraction, x-ray photoelectron spectroscopy, ultraviolet photoemission spectroscopy, ion-scattering spectroscopy, and scanning Auger microscopy. Overlayer characteristics are examined at substrate temperatures of 300 and 600 K. We find that the equilibrium configuration is not predicted by any of the three traditional growth modes (Frank-Van der Merwe, Stranski-Krastanov, or Volmer-Weber). Rather, the equilibrium film structure is that of a Ag-Rh-Ag sandwich, most probably flat. Formation of the sandwich is thermodynamically driven by the difference in surface free energies between Ag and Rh, and is kinetically accessible because of the high mobility of the Ag atoms.

INTRODUCTION

In recent years there has been a tremendous increase in the number of investigations of metal-on-metal systems. Interests have ranged from fundamental studies of epitaxy to catalytic studies of bimetallics (e.g., Refs. 1-3). In most studies the motivation has been to determine the influence of the substrate on the properties of the overlayer film. To fully understand these substrate-overlayer interactions one must first know the structure of the overlayer film. Therefore, many efforts have focussed on overlayer growth and the way in which electronic properties depend on the structure of the overlayer.

Most metal-on-metal studies are approached with the expectation that the film will grow in one of the three classical modes:⁴ sequential filling of layers (Frank-van der Merwe mode); agglomeration into three-dimensional crystallites (Volmer-Weber mode); or growth of one or more layers followed by agglomeration (Stranski-Krastanov mode). The equilibrium growth mode in these systems is thought to reflect a balance between three thermodynamic factors: the surface free energy of the film γ_f , the surface free energy of the substrate γ_s , and the interfacial energy γ_i . It is often beneficial to have ordered layer growth, e.g., layer growth is desired when studying the electronic states of metal overlayers because this makes it possible to model the substrate-overlayer system.⁵ For this reason, as well as for practical reasons of ease of preparation, substrate-overlayer combinations are often chosen such that $\gamma_f \lesssim \gamma_s$. However, recent interest in the area of ferromagnetism has led to work on systems such as Fe/Cu,⁶⁻¹¹ Fe/Au,¹² and Fe/Ag,¹³ and

the interesting catalytic properties of Pt-Au alloys have motivated studies of the system Pt/Au.¹⁴ These are all systems where $\gamma_f > \gamma_s$ and γ_i is expected to be small and often positive. For these systems, Bauer's criteria predict Volmer-Weber growth.⁴

The present work concerns a system somewhat analogous to Fe/Cu and Fe/Ag in terms of free energies: Rh/Ag(100). The surface free energy of Rh, 2.83 J/m², is more than twice that of Ag, 1.30 J/m²,¹⁵ and so one would expect three-dimensional clustering of the Rh film here as well. However, we find that the equilibrium configuration of the film falls outside of the three classical modes. Our results indicate that the overlayer structure depends on additional factors which may also be relevant in some analogous systems where controversies have arisen.^{8,9,11}

EXPERIMENT

The experiments are performed in three separate ultrahigh-vacuum systems. One chamber is equipped for ultraviolet photoemission spectroscopy (UPS), x-ray photoelectron spectroscopy (XPS), and ion-scattering spectroscopy (ISS). A second chamber is equipped for thermal-desorption spectroscopy (TDS). Both of these systems have base pressures $\leq 2 \times 10^{-10}$ Torr and are equipped with optics for low-energy electron diffraction (LEED) and Auger-electron spectroscopy (AES), shuttered Rh evaporators, and provisions for CO exposure. The sample manipulators allow for resistive heating, from 120 up to 1000 K for TDS, and from 300 to 1000 K for UPS, XPS, and ISS measurements. Scanning Auger mea-

measurements are performed in the third chamber, a Perkin-Elmer PHI 600 scanning Auger system, operating in the high 10^{-10} to low 10^{-9} Torr range.

The Ag samples, flat disks approximately $10 \times 10 \times 2$ mm³ in size, are cut from the same single-crystal boule, oriented parallel to the (100) face to within $\pm 0.5^\circ$, and polished by standard metallurgical procedures. Sulfur is the only bulk contaminant observable by AES and is removed by repeated argon-ion bombardment at 500 eV ($\approx 2 \mu\text{A}/\text{cm}^2$) and annealing to 800 K. The surface region is determined to be free of sulfur when prolonged heating (1–2 h) at 800 K results in a sulfur signal which is undetectable with AES. After annealing at 800 K, LEED shows the characteristic (1×1) pattern.

Rh is deposited on the sample surface from a resistively heated, tungsten filament wrapped with 0.25-mm-diam Rh wire (99.8%), following the design of DeCooman and Vook.¹⁶ The Rh source is enclosed in a double-walled, liquid-nitrogen-cooled shroud with a 1.5-cm orifice to allow Rh vapor to escape toward the sample. After thorough outgassing of the filament, the pressure rise in the chamber is about 4×10^{-10} Torr after 60 sec. No impurities are detectable in the deposited Rh overlayer using either AES or XPS. From AES, the Rh distribution across the sample surface is uniform to within $\pm(5-10\%)$. The Rh is removed by argon-ion bombardment after each experiment. The conditions of bombardment are 1 keV, $\sim 4 \mu\text{A}/\text{cm}^2$ at 300 K.

RESULTS

Our initial investigations involved monitoring the growth of the film via AES, XPS, $\Delta\phi$ (work-function change), and LEED measurements at a substrate temperature of 300 K. It is common to characterize film growth using AES by monitoring the overlayer and substrate signal intensity versus deposition time (e.g., Ref. 17). Accordingly, we measure the Ag_{356} eV (*MNN*) and Rh_{222} eV (*MNN*) Auger transitions. The results are shown in Fig. 1. It can be seen that the measured peak-to-peak ampli-

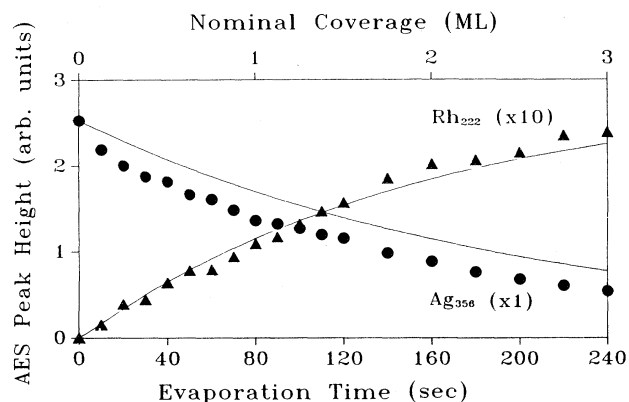


FIG. 1. Variation of the differentiated Rh_{222} eV and Ag_{356} eV Auger signal intensities with deposition time during Rh deposition on $\text{Ag}(100)$ at 300 K.

tudes of the derivative spectra, plotted as functions of deposition time, are smooth, continuous curves, with no clear changes in slope. The AES data are thus ambiguous in their meaning, since they fail to exhibit the clear straight-line segments, with discontinuities in slope, which are often associated with sequential layer filling.^{18–20} The absence of such a form in Fig. 1 does not rule out layer-by-layer growth, however.²¹

An absolute determination of Rh coverage is difficult. This is because the Auger data (Fig. 1) do not exhibit clear linear segments which demarcate various layers, and because we have no experimental way to monitor the absolute Rh flux from the evaporator. However, we estimate the Rh coverage by assuming that growth is pseudo-layer-by-layer at 300 K. The nominal coverages given in Fig. 1 are based on ion scattering results which indicate that after an 80-sec exposure to the Rh source the Ag surface atoms are approximately 70% covered. Such a value is consistent with pseudo-layer-by-layer or nondiffusive growth processes^{22,23} in which the second layer begins to populate before completion of the first. Also included in Fig. 1, and represented by the solid lines, are the curves calculated for the Ag_{356} eV signal attenuation and the Rh_{222} eV signal increase assuming layer-by-layer growth as suggested by Gallon.¹⁸ We assume the interlayer spacing in the Rh film is the same as for bulk Rh, 1.90 Å, and use inelastic mean free paths calculated from the equations of Seah and Dench.²⁴ Subsequent coverage values given are based on this data.

Figure 2 illustrates the work-function change $\Delta\phi$ measured from the shift in the low-kinetic-energy cutoff of the He I photoemission spectrum. The work function increases smoothly (by ~ 0.5 eV) as Rh, three layers, is deposited at 300 K. Measurements of $\Delta\phi$, using a retarding potential method,²⁵ similarly show a smooth increase (~ 0.7 eV). These data are also shown in Fig. 2. Both measurements are consistent with the higher work function of $\text{Rh}(100)$ relative to $\text{Ag}(100)$: 5.11 eV (Ref. 26) versus 4.65 eV (Ref. 27), respectively.

Finally, the LEED pattern shows an increase in back-

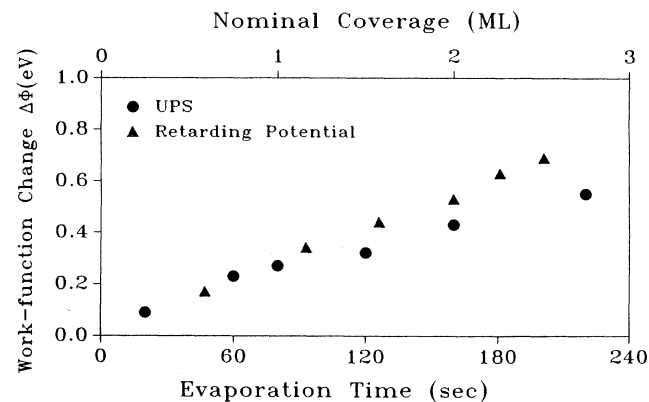


FIG. 2. Variation of work function during deposition of Rh films at 300 K, as measured by UPS and a retarding potential method.

ground intensity with subsequent deterioration and loss of the (1×1) pattern during Rh deposition. The LEED pattern is obliterated at a coverage of ~ 1 Rh layer. There is no evidence of LEED oscillations, as we have observed during growth of Pt films on Pd(100).²⁸⁻³⁰ These oscillations would be indicative of layer-by-layer growth.

It is often believed that the equilibrium configuration of the overlayer can be attained by annealing a film deposited at room temperature. When a fresh Rh film is heated to 600 K, a very diffuse (1×1) LEED pattern returns, indicating that some ordering of the overlayer has occurred. The spacing of the large diffraction spots is most consistent with the bulk lattice constant of Ag at low-Rh coverages, and with that of Rh at high-Rh coverages. In addition, gross changes in the system are evident, as illustrated by the AES data of Fig. 3. XPS data (not shown) indicate a similar result. In both cases, the Rh signal shows a striking decrease in intensity while the Ag signal intensity increases appreciably. Observation of such spectral changes could, in principle, be due to loss of the film via bulk dissolution and/or agglomeration of the film from flat layers into three-dimensional clusters. However, Rh should be completely insoluble in Ag in this temperature regime,³¹ and so we do not consider the first explanation to be feasible. Since agglomeration would be expected to occur upon equilibration due to the difference in surface free energies of Rh and Ag, we initially adopted the latter explanation as the more likely. A similar effect has been reported for Pd films on W(110), where the film grows layer-by-layer at room temperature but agglomerates at higher temperatures, resulting in a loss of Pd intensity relative to W.³²

However, additional data are not consistent with the simple hypothesis of Rh agglomeration. Annealing a Rh

overlayer not only causes a loss of Rh spectral intensity but also causes ϕ to drop close to the value of clean Ag, and completely poisons the surface to CO chemisorption. This latter effect is observed by measuring CO uptake at high exposures, 20 L, using both UPS and TDS. [1 langmuir (L) $\equiv 10^{-6}$ Torr sec.] In these experiments He II UPS indicates that CO adsorbs molecularly on all Rh films.

The TDS data are illustrated in Fig. 4. In these measurements the sample is exposed to 20 L CO at ~ 120 K, then the temperature is ramped upward while measuring the partial pressure of CO. Curve (a) shows the result for clean Ag(100), and curve (b) shows the result after approximately 4 monolayers of Rh are deposited at 120 K. There is a single major desorption peak at ~ 470 K, which completely disappears after the film is annealed to 600 K, curve (c). Thermal desorption of CO from pure Ag occurs at very low temperatures, below ~ 120 K,³³ whereas the desorption from Rh is known to take place with maximum rates between 500 and 570 K.³⁴⁻³⁷ We thus attribute the peak at 470 K in Fig. 4 curve (b) to desorption of CO from Rh. We believe that desorption below 200 K in these spectra is largely due to sample heating wires and other manipulator parts, rather than desorption from Ag. These TDS data, combined with the UPS and $\Delta\phi$ measurements, lead us to believe that an Ag layer diffuses to the Rh surface upon annealing, thus poisoning the surface to CO chemisorption.

The data of Fig. 5 support this hypothesis. Figure 5 shows results from an experiment in which the annealed Rh film is slowly argon-ion etched, ≈ 0.02 – 0.03 monolayer/min, while monitoring the Rh and Ag Auger signal intensities, $\Delta\phi$, and CO uptake. This experiment is performed on a Rh film about three layers thick, deposited at 300 K, annealed to 600 K for 15 min, and cooled to

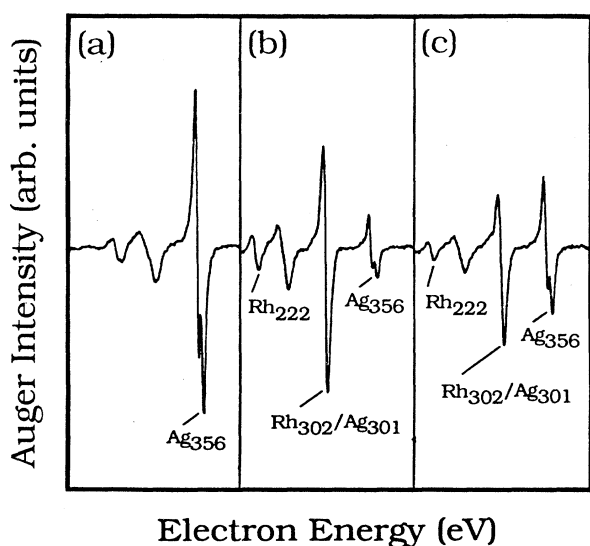


FIG. 3. Auger spectra in the energy range 200–400 eV. (a) Clean Ag(100). (b) Following deposition of approximately three layers of Rh at 300 K. (c) As in (b) following heating to 600 K.

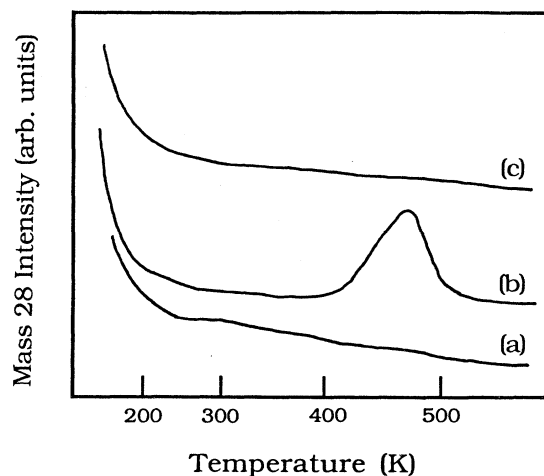


FIG. 4. Thermal desorption of CO. (a) Following exposure of clean Ag(100) to 20 L CO at 120 K. (b) Following deposition of approximately four Rh layers on Ag(100) at 120 K, followed by exposure to 20 L CO at 120 K. (c) Following the experiment of curve (b). Note that at the end of that previous experiment, the sample was heated to 600 K.

300 K. For the as-deposited and annealed data points indicated, the Auger ratio and work-function change were measured first, followed by saturation of the surface by a 20 L CO exposure and measurement of the CO uptake via the CO 4σ peak area of the He II photoemission spectrum. Each successive point thereafter represents the same sequence of measurements taken after argon-ion etching to remove the CO and underlying surface atoms. The depth profiles of Fig. 5 clearly show that the surface has become Ag-rich upon annealing. This Ag layer can be removed to reveal a Rh-rich layer with properties very similar to the fresh Rh film. However, it is evident that the $I(\text{Rh})/I(\text{Ag})$ Auger ratio and CO uptake never quite return to the same values as for the freshly deposited film at 300 K. This is most likely due to the presence of some Ag mixed in with the Rh, either as a result of the ion etching or the annealing treatment itself. The higher value of $\Delta\phi$, as deposited at 300 K and after sputtering is thought to result from background CO adsorption, which is known to increase the work function by as much as 1.2 eV at coverages of 0.60 monolayers on Rh(100).²⁶

He-ion-scattering experiments provide further support for this picture. We find that dosing an unannealed, Rh-covered surface with CO completely attenuates all the

metal scattering signal intensity, i.e., adsorbed CO completely occludes all the Rh sites. Since CO will not stick to Ag at 300 K, this provides a means for detecting the presence of Rh at the surface of an annealed overlayer by looking for a decrease in signal intensity when CO is adsorbed. The results of this experiment, performed using a 1-keV incident ion beam with the system back filled to a pressure of 5×10^{-6} Torr He, are shown in Fig. 6. These spectra are taken with an aperture (12°) double-pass cylindrical minor analyzer (CMA) (with appropriate potentials reversed), the ions are scattered through an angle of 150° . The ions are incident on the surface at an angle of 72° with respect to the surface normal. For clean Ag(100), the scattered He ions have an energy of 850 eV, as seen in Fig. 6(a). After deposition of about three layers of Rh, the spectrum of Fig. 6(b) is acquired. The scattering from Rh also occurs at 850 eV due to the poor energy resolution of He for high-mass atoms. The reduction in scattered intensity is believed to result from some disorder in the film surface, as indicated also by LEED measurements, and/or attenuation from gas adsorption rather than a large difference in scattering coefficients or neutralization efficiencies. When this surface is exposed to CO, the peak at 850 eV disappears as shown in Fig. 6(c). The peak at 380 eV in this spectrum is a result of He scattering from the oxygen of the adsorbed CO molecules. The ISS spectrum after annealing to 600 K is shown in Fig. 6(d). It is clear that there is a large recovery of the peak at 850 eV. Dosing again with 20 L of CO and repeating the scattering experiment has no effect on the peak height, indicating that all the Rh sites have been completely covered with Ag. This is also suggested independently from the absolute peak intensities of Figs. 6(a) and 6(d), which are identical within experimental error. These data show that there is Rh exposed at the surface of the film deposited at 300 K and that Ag

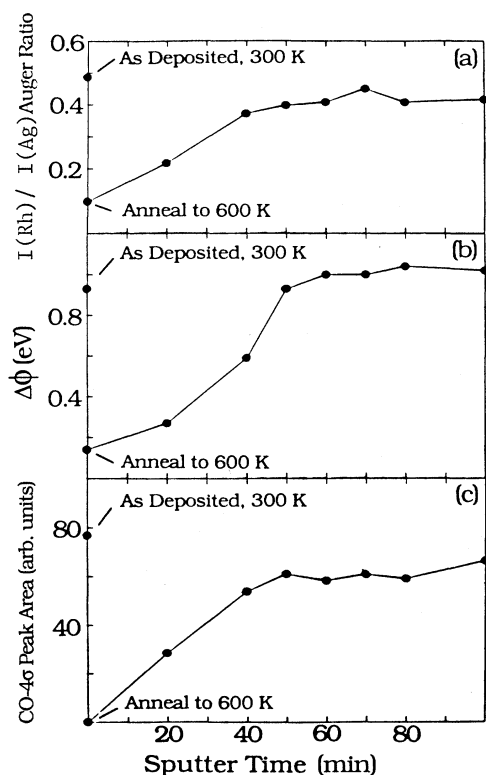


FIG. 5. Measurements of $I(\text{Rh})/I(\text{Ag})$ Auger intensity ratio (top), work-function change (middle), and CO- 4σ peak area (bottom) while a Rh film, approximately three layers deep and annealed to 600 K, is argon-ion etched (1 keV, 1×10^{-6} Torr Ar) at 300 K.

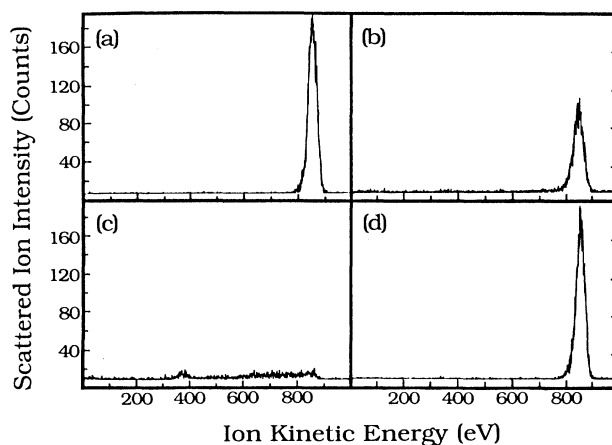


FIG. 6. Ion-scattering spectra taken with a rastered ($\approx 1 \text{ cm}^2$) 1-keV ion beam at 5×10^{-6} Torr He. (a) Clean Ag(100). (b) Following deposition of approximately three layers of Rh at 300 K. (c) As in (b), followed by exposure to 20 L of CO at 300 K. (d) As in (c), following heating to 600 K.

covers the surface upon annealing to 600 K. This is in complete agreement with the results from TDS.

We estimate the thickness of the top Ag layer to be one to two atoms. This depth is consistent with the conditions required to sputter through the top Ag layer, assuming a sputtering yield of unity. This value is also suggested, independently, from the ratio of $I(\text{Rh})/I(\text{Ag})$ Auger intensities, 0.10, which we obtain after annealing very-thick-Rh layers, about 16 layers deep. For one and two monolayers of Ag on Rh(100), this ratio is known to be 0.25 and 0.09, respectively.³³ The LEED data indicate that, at low-Rh coverages, the top Ag layer adopts approximately the same lattice constant as bulk Ag (and the Rh must follow suit), whereas for thick-Rh films, both the Rh and Ag adopt the two-dimensional lattice constant of bulk Rh.

Several experiments, including AES, ISS, and TDS, have been used to ascertain more precisely the conditions under which Ag moves to the Rh surface. The AES data are shown in Fig. 7, where the sample is heated at a rate of 1–2 K/sec with successive 60-sec pauses at each temperature to record the Auger spectrum. The $I(\text{Rh})/I(\text{Ag})$ Auger intensity ratio is shown as the ordinate. The abrupt decrease in this ratio reflects the onset of Ag migration to the surface. It can be seen that when the initial coverage of Rh is about 1 monolayer, Ag migration occurs at ~ 360 – 380 K, whereas at higher coverages (up to 4 monolayers) it begins at ~ 420 K. Another interesting aspect is the fact that the final ratio of Rh:Ag intensities always approaches the same value, 0.1, for all initial Rh coverages above approximately 1 monolayer.

ISS can be used to study this phenomenon as well, by exploiting the ability to mask ion scattering from the surface Rh atoms using adsorbed CO. This is accomplished by saturating a fresh Rh deposit with CO, and then monitoring the intensity of the He ion-scattering peak at 850 eV as a function of temperature. The result of this experiment is shown in Fig. 8, for an initial Rh coverage of ~ 3 monolayers. This measurement indicates that Ag begins

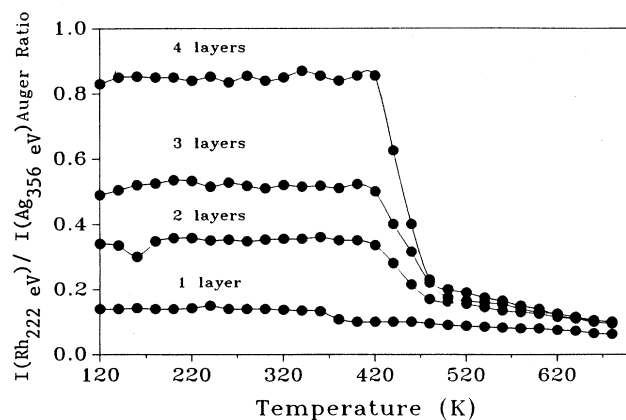


FIG. 7. Variation of $I(\text{Rh})/I(\text{Ag})$ Auger intensity ratio as a function of sample temperature, for several initial coverages of Rh as deposited at 120 K.

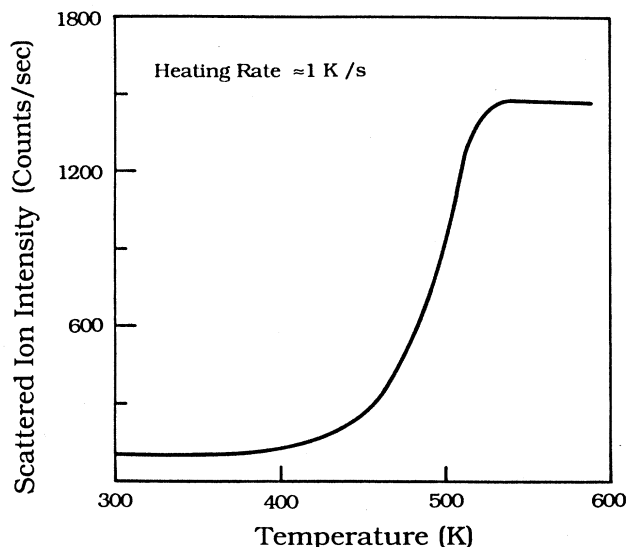


FIG. 8. Intensity of the He-ion-scattering peak at 850 eV as a function of temperature. (1 keV at 5×10^{-6} Torr He, 1 cm^2 raster.)

to appear at the surface at about 400 K, slightly lower than the onset determined with AES. This is most probably due to the higher surface sensitivity of the ISS experiment.

It is useful to compare the ISS and AES data with the TDS results, shown as a function of Rh coverage in Fig. 9. The onset of desorption for the three-layer film of Fig.

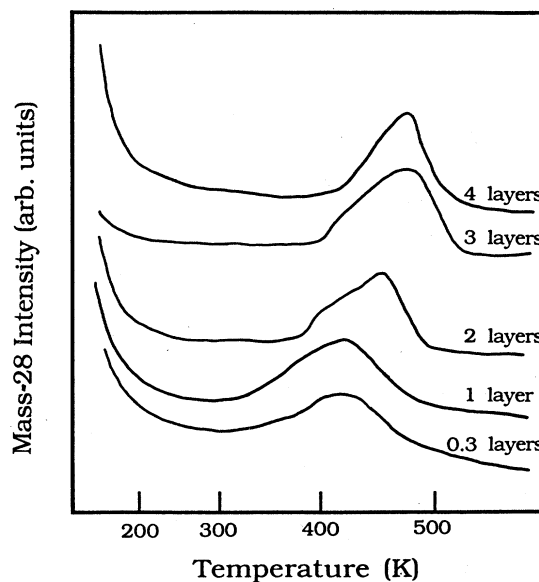


FIG. 9. Thermal desorption of CO from Rh films deposited at 120 K and exposed to 20 L CO at 120 K. Each curve represents a different initial coverage of Rh.

9, 400 K, is identical within experimental error to the temperature at which the ion scattering intensity first increases, and the peak temperature corresponds to the inflection point of the ISS curve of Fig. 8. Combining the AES, ISS, and TDS data allows us to conclude that the desorption of CO is not a simple unassisted event, but rather CO is being displaced by diffusing Ag. These observations explain the low temperature at which the CO desorption peak maximum occurs, 30–100 K lower than for the surfaces of bulk Rh.^{34–37}

The temperature of CO desorption shifts upward as Rh coverage increases in Fig. 9. Both the desorption onsets and the desorption peak maxima move to higher temperatures. The TDS measurements reveal that these increases must reflect an increase in kinetic limitations for diffusion by Ag, in the case of the thicker film. This suggests that the mechanism for Ag diffusion is somewhat different at low-Rh coverages than at higher-Rh coverages. A reasonable scenario is one in which bare patches of silver are exposed at low-Rh coverages, so the migration of Ag to the Rh surface involves simple lateral migration. However, at higher-Rh coverages the Ag must break through a more contiguous Rh film, and this is more difficult. This mechanism is illustrated schematically in Fig. 10.

Auxiliary measurements, obtained by transferring the sample to a scanning Auger microscope (SAM), lend support to the diffusion mechanism described in Fig. 10. A fresh Rh film, ~16 layers deep, is deposited and annealed to 600 K for 30 min in order to bring the Ag to the surface. The sample is then transferred (in air) to a SAM instrument. Initial measurements show that after exposure of the sample to atmosphere, the surface is predominantly Rh, with only a small amount of Ag still detectable. Sulfur and carbon are also present. Apparently, the Rh must have a higher affinity for the contaminant species, and the Ag is thus driven back off the surface.

Only after removal of the contaminants by ion etching does Ag migrate back to the surface. This migration is

again found to occur at about 380 K. We are fortunate, in that the secondary-electron yields for Rh and Ag are sufficiently different so that the Ag can be monitored visually in this device as it migrates to the surface. A series of time-lapse micrographs, indicating the evolution of the Ag layer at the surface, is shown in Fig. 11. Figure 11(a) is a micrograph of the carbon- and sulfur-contaminated surface while it is held at 380 K. No changes in surface composition are evident even after several hours at this temperature. When the surface is lightly ion etched to remove the contamination, Ag spreads almost immediately out onto the surface. This is evident in Fig. 11(b), which is taken in the first 60 sec after turning the ion beam off. The sample temperature is maintained constantly at 380 K. The diffusing Ag shows up as light spots on the darker Rh background. The changes are even more pronounced in Fig. 11(c), taken 15 min after sputtering. It must be noted that the changes in the micrographs are due to changes in elemental composition of the surface layers, not changes in topography.

The diffusion of Ag appears to begin at randomly dispersed point sources and then slowly spread out over the surface. The Ag does not seem to emerge uniformly, as would be envisioned for surface segregation from an equilibrium alloy. Auger spectra taken from the Ag patches indicate again that the Ag is only one to two atoms deep. A lower-magnification picture of the same area, Fig. 11(d), shows that the size of Ag islands are mostly uniform, except for a few larger patches. The larger Ag islands could result from faster diffusion through larger defects or possibly through thinner areas of the film. The firm conclusion that we can reach, however, is that the Ag appears to spread outward from randomly distributed, point sources, rather than emerging uniformly across the surface.

Some insight into the structure of the Rh films, and the way in which this structure depends upon temperature, is provided by XPS. These data are shown in Fig. 12. It can be seen that the Rh binding energy (BE) increases with deposition time at 300 K, which undoubtedly reflects the increase in average atomic coordination of Rh atoms as the bulk configuration is approached.³⁸ This trend is evident for submonolayer to ~3–4 monolayers of Rh. The Ag binding energy decreases continuously, in a way which is independent of the film's thermal history. The decrease of the Ag BE must be due to an increase in the contribution from the less-highly-coordinated Ag at the interface or at the surface and concurrent attenuation of signal from the bulk Ag as Rh coverage increases. A more puzzling result is the fact that there is no measurable change in Rh BE when a Rh overlayer, deposited at 300 K, is annealed to 600 K. This is true for low (< one layer) as well as high coverages (three to four layers) of Rh. On the other hand, when a Rh film is deposited at 600 K, the shift in BE for fixed deposition time is smaller than at 300 K. These results are shown also in Fig. 12. In other words, the BE shift depends quite strongly on the history of the film; annealing to 600 K has a much different effect than depositing at 600 K. There are two possible explanations for this. One is that the composi-

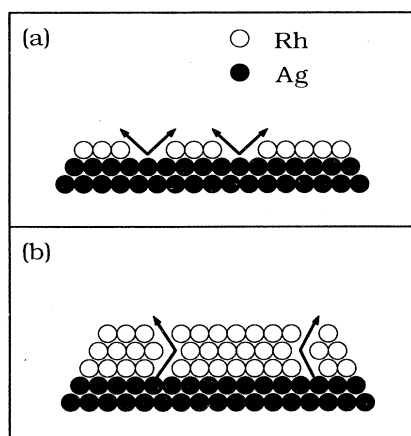


FIG. 10. Schematic model of Ag diffusing to coat the Rh film. (a) Low-Rh coverages; (b) high-Rh coverages.

tion of the Rh layer is different in the two cases. More intermixing of Ag with Rh may occur when Rh is deposited at the higher substrate temperature, thus leading to a decrease in the Rh BE. This intermixing could be due to the high mobility of Ag at 600 K, which allows it to constantly migrate toward the surface and be buried by the incoming Rh atoms. Another explanation is that the morphology of the films is different in the two cases. If the film deposited at 300 K is significantly rougher than the one grown at 600 K due to limited Rh diffusion at the lower substrate temperature, this would be consistent with the data as well. However, one would then have to conclude that annealing a rough film to 600 K does not allow it to become more smooth. This would be reasonable, since cooperative, large-scale rearrangement of an already-rough film would undoubtedly be relatively difficult and may simply not occur on the time scale of our annealing experiments. Homoepitaxy experiments may be a possible means of ascertaining experimentally whether Rh is much more mobile at 600 K than at 300 K.

The XPS data lead us, then, to conjecture that the content of the middle Rh layer may depend upon the film's

history. To test this hypothesis, depth profiles (sputtering rate $\approx 0.1\text{--}0.2$ monolayer/min) were performed with AES, following different thermal treatments. Figure 13 shows the results of these profiles for films about three layers thick. There is obviously little difference between the profile of the film heated to 600 K, Fig. 13(b), or that of the film deposited at 600 K, Fig. 13(c). The change in composition needed to bring about the observed difference in Rh BE is unknown, and it may be so small that we cannot differentiate between the two in the profiles. In addition, the ion beam used in the depth profiling tends to roughen and mix the interface, making it difficult to distinguish small changes in the concentration profiles. However, we conclude that the differences in film composition, if present, are relatively small (less than about 20%). The Rh signal remaining after 60 min of sputtering can be explained by the overlap of the Rh_{302 eV} transition (used to monitor the Rh concentration) and the Ag_{301 eV} transition, and/or Ar-ion mixing or knock-on from the sputtering process.

If there is intermixing between the two metals in the middle layer, we do not believe that this reflects significant alloy formation. We have measured the

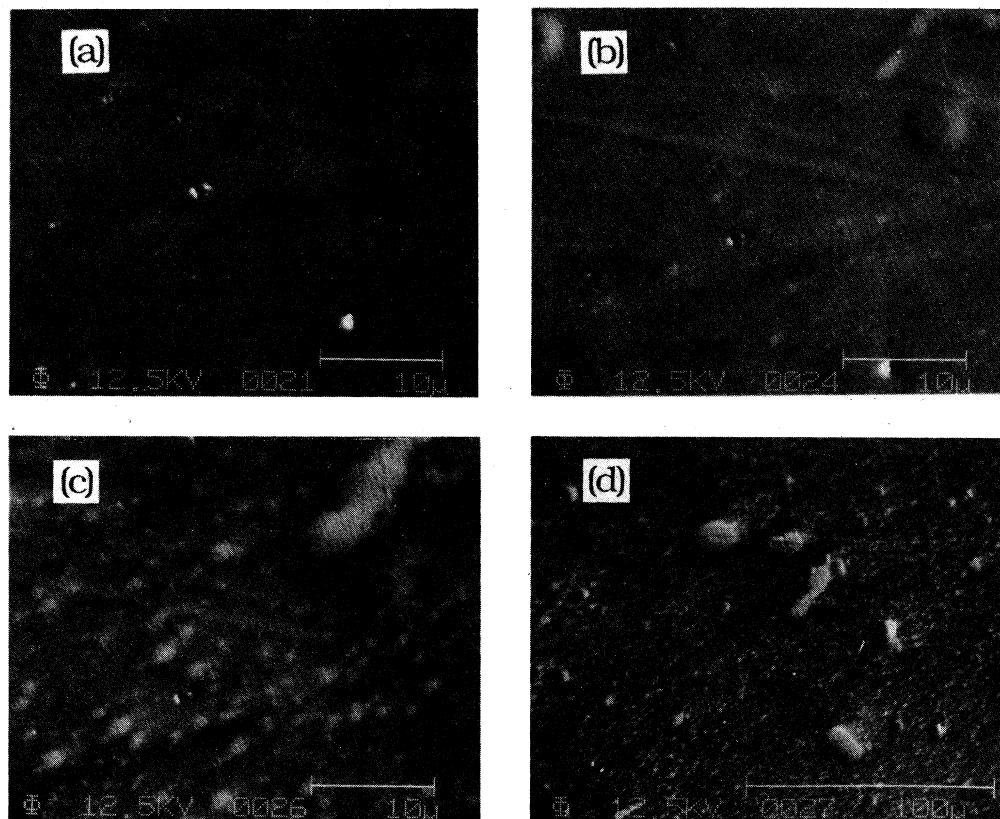


FIG. 11. Electron micrographs of a thick, ≈ 16 -layer Rh film. Sample temperature is held at 380 K. (a) Carbon- and sulfur-contaminated surface (2510 \times). (b) As in (a), ion-etched to remove the carbon and sulfur, 60 sec after turning off the ion beam (2510 \times). (c) As in (b), 15 min after turning off ion beam (2510 \times). (d) As in (c), magnification of 508 \times .

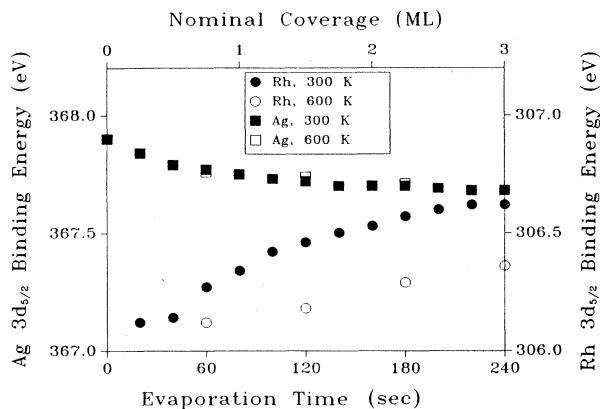


FIG. 12. Variation of core-level binding energies (BE), measured with XPS using Mg $K\alpha$ radiation, for both Rh and Ag as a function of deposition time during growth of Rh films.

angle-integrated, He II, UPS spectra for the Rh/Ag films, both before and after annealing. These spectra are shown in Fig. 14. Alloying may be accompanied by a mixing or hybridization of states which can give rise to new features of shifts in the existing features of the valence-band density of states. Such effects have been observed, for in-

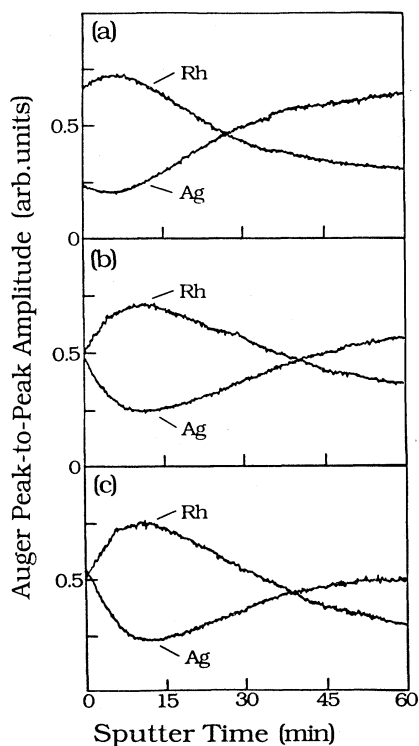


FIG. 13. Depth profiles, using the peak heights of the differentiated Rh_{302 eV} and Ag_{356 eV} Auger transitions, for Rh films which have undergone various thermal treatments. (a) Three layers of Rh deposited at 300 K. (b) Three layers of Rh deposited at 300 K, then annealed to 600 K for 15 min. (c) Three layers of Rh deposited at 600 K.

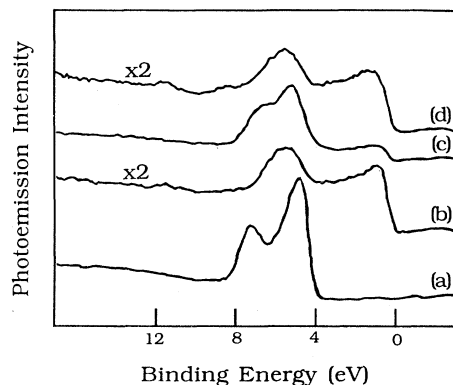


FIG. 14. Angle-integrated He II photoemission spectra of the 4d-band region of the valence band, taken with a He resonance source. (a) Clean Ag(100). (b) Following deposition of approximately three Rh layers at 300 K. (c) As in (b), following heating to 600 K. (d) As in (c), sputtered to remove the top Ag layer.

stance, in the systems Pd/Cu,^{39,41} Pd/Ag,²⁷ and Cu/Au.⁴² The data of Fig. 14 show that the spectra for Rh/Ag are just a superposition of the bulk Rh and Ag d -band spectra, both before and after annealing. This data is not to be taken as unequivocal evidence against alloy formation since alloying may result in only small changes in the density of states, especially for dilute alloys, and may not be observable in these spectra.

Another question about the structure of the film is whether any Ag is present at the surface following Rh deposition at 300 K, i.e., before any annealing. None of the data presented until now would be sensitive to small amounts of Ag at the surface under these conditions, including the ISS. In Fig. 13(a), however, the profile of the unannealed Rh film shows an initial decrease in the Ag intensity, indicating some small surface enrichment in Ag. This shows that even at room temperature, Ag has enough mobility to diffuse (slowly) onto the top of the Rh. However, the rate at which the Rh film is grown and the moderate temperature of the substrate serve to kinetically limit the diffusion process, and the equilibrium configuration is only reached on a reasonable time scale after annealing the system.

A final question about the nature of the film is, what is its three-dimensional structure? Is it largely smooth, or does the Rh form three-dimensional crystallites? The best available answer to this question is given by the AES data shown in Fig. 15. As mentioned earlier, the $I(\text{Rh})/I(\text{Ag})$ Auger intensity ratio for an annealed film of ≈ 16 layers is 0.1. This same ratio is obtained for all films thicker than two to three layers, whether they are annealed to 600 K after deposition, or grown at 600 K. This is evident in the data of Fig. 15. For films grown at 600 K this ratio plateaus at a coverage of about three to four Rh layers. For a 16-layer film the coverage is ≈ 4 times that required to completely attenuate the substrate signal, and Ag is detected only after the film is annealed. For the unannealed, three-layer film the Ag signal intensity is still 20% of the clean substrate signal, yet after an-

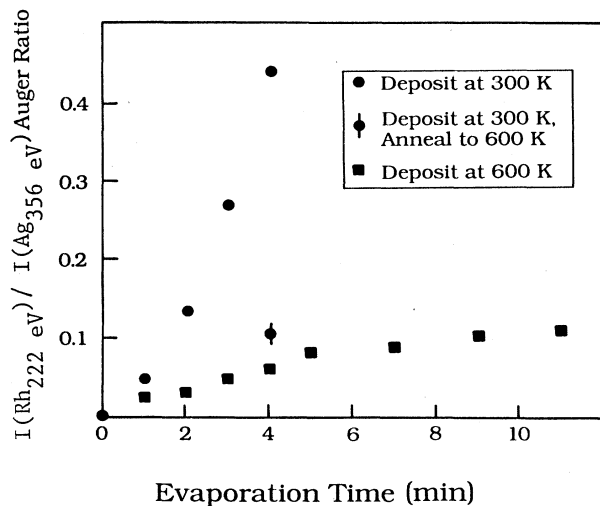


FIG. 15. AES ratio during film deposition at 300 K (approximately three layers) and 600 K (approximately nine layers).

nealing the Rh/Ag ratio is identical to that of an annealed 16-layer film. If the Rh does agglomerate upon heating, the Rh:Ag ratio should still increase with increasing Rh coverage, only at a lesser rate, and plateau only when the crystallites have grown large enough to coalesce and completely attenuate the substrate Auger signal. It is difficult to envision how the Auger ratio for three- and 16-layer annealed films could possibly be identical, if significant agglomeration occurs upon annealing. However, for a flat Rh overlayer with a layer of Ag on the surface, the constant Auger ratio for the large range of Rh coverages is more easily explained.

This second explanation of the identical Auger ratio is also reasonable, in light of the attenuation of Ag Auger electrons emitted from the substrate. Assuming the thickness of an ordered, flat Rh monolayer to be bounded by the values for the interlayer spacings of bulk Rh and Ag (100) planes, 1.90 and 2.05 Å, respectively, and using an inelastic mean free path of 7.0 Å, the attenuation length of the Ag_{356 eV} electrons should be approximately four monolayers. A Rh film of three layers which has been annealed to bring a layer of Ag to the surface results in a total coverage of 4 monolayers, approximately the attenuation length of the Ag_{356 eV} Auger electrons. This would indicate that the majority of the electrons contributing to the measured Auger signals originate from layers above the Ag substrate/Rh interface for all Rh coverages greater than three layers. Therefore if the Rh layers remain flat, and the concentration of Ag dispersed throughout the Rh and at the surface remains essentially constant, for all Rh coverages, a constant Rh/Ag ratio would be expected for films greater than about three layers. This seems to be a more acceptable explanation for the constant Auger ratio than agglomeration. Our AES data thus seem to support the formation of a flat Ag-Rh-Ag sandwich.

DISCUSSION

The following picture emerges from the data of the preceding section.

Structure of the metallic film. The equilibrium structure of a Rh film on Ag(100) is that of a Ag-Rh-Ag sandwich. The top Ag layer is only one or two atoms deep, and it completely blankets the Rh. The energetic driving force for this silver migration is undoubtedly the reduction in the system's surface free energy, which is accomplished by this very thin layer of Ag. However, the Ag layer is also highly strained, especially at high Rh coverages, since our LEED data indicate that it adopts the lattice constant of the Rh substrate, 8% lattice mismatch. This creates an unfavorable energy term in the total energy balance, a term which apparently dominates at coverages above one or two atomic layers of Ag. This strain energy may also prevent more Ag from moving to the surface.

It is informative to compare our results with work of Peebles *et al.*³³ in which Ag films on Rh(100) were studied. Those authors find that Ag grows layer-by-layer up to at least three atomic layers at 300 K, and follows Stranski-Krastanov growth at 640 K, close to the annealing temperature of many of our experiments. They report that clustering begins during Stranski-Krastanov growth at coverages in excess of 1 monolayer. They also find that the film grows epitaxially up to a coverage of 1 monolayer at 300 K, but reconstructs into a pseudohexagonal lattice at higher coverage. Both of these findings suggest that Ag coverages above 1 monolayer cannot accommodate the 8% lattice misfit with the Rh substrate, and either reconstruct (at 300 K) or agglomerate (at 640 K) to relieve the strain. To the extent that our Rh films are electronically and structurally similar to their Rh(100) substrate, their results can be extrapolated to our system. This suggests that the top layer of our sandwich is probably limited to a single Ag atom in thickness.

The middle layer of the sandwich is mainly Rh. The bimetallic phase diagram³¹ indicates that a dilute Rh-Ag alloy, consisting of ≤ 5 at. % of Ag, exists at room temperature, and so there may be a small amount of Ag truly dissolved in the Rh layer. However, this possibility is disfavored by the results of Peebles *et al.*,³³ who find no evidence for dissolution of Ag into Rh(100), even at temperatures up to 1370 K. Presumably, the detection limit in their AES experiments is on the order of 1% or 2%. There may be some pure Ag phase trapped in our Rh films, especially those grown at elevated temperatures. This is because the Ag tends constantly to migrate toward the surface as the film is being grown at elevated temperature, and some of it may become buried within the growing film.

We believe that the substrate is pure Ag, with no dissolved Rh. We have no experimental data to this effect, but the phase diagram³¹ indicates that less than 0.5 at. % of Rh is soluble in Ag at room temperature. Thus, we propose that the layers of this sandwich are rather pure, with some metallic intermixing in the middle layer, but none in the top and bottom layers.

For the reasons given in the third section, we believe

that the Ag-Rh-Ag sandwich is essentially flat. In this case, Rh films thicker than 1 monolayer must develop misfit dislocations in order to accommodate the 8% lattice mismatch between the Rh and the Ag. The misfit dislocations presumably account for the diffuse nature of the (1×1) LEED pattern which we observe for the annealed films, even for thick-Rh sandwiches.

The morphology of the Rh films grown at 300 K, where silver migration is slow on the time scale of our experiments, is also questionable. The sharp (1×1) LEED pattern of the substrate is obliterated after one layer of Rh is deposited at room temperature, which may indicate that the Rh atoms are randomly and uniformly distributed over the surface. If significant agglomeration occurred under these conditions, one might expect the underlying Ag substrate to give a residual LEED pattern even at much higher Rh coverages. It may be that the film grows via random deposition of Rh atoms, and that thermal diffusion is slow at 300 K. In this case, the growing film would be rough, yet would have some layer-by-layer quality, especially for the first 2–3 monolayers. The observation of layer-by-layer quality in films grown at temperatures where single-atom diffusion is negligibly slow has been a topic of some recent discussion.^{23,29,30,43–45}

Mechanism of Silver Migration. The data presented clearly show the ability of Ag to migrate to the surface of a Rh film, the kinetics of this process depending on the substrate temperature and the film thickness. The exact mechanism which leads to the sandwich structure is not clear. It is well known that binary alloys often show a tendency for surface enrichment or segregation of one of its components. Many theories exist which can be used to predict the surface segregation of transition-metal alloys.^{46,47} These theories predict the segregation of Ag in the Rh/Ag system. Therefore it is possible that the sandwich forms as a result of the segregation of Ag from a dilute Rh-Ag alloy. However, SAM results indicate that the Ag diffusion appears to begin at randomly dispersed point sources and then slowly spreads out over the surface. The Ag does not seem to emerge uniformly as would be envisioned for surface segregation from an equilibrium alloy.

There exists a more plausible explanation for the development of the Ag-Rh-Ag sandwich, as illustrated previously in Fig. 10. The migration of Ag at low-Rh coverages may involve simple lateral migration of Ag atoms from bare patches of the substrate. This is easy to envision. However, at higher-Rh coverages the Ag must break through a more contiguous Rh film. For these higher-Rh coverages it is possible that Ag arrives at the surface via diffusion through defects which may exist in the overlayer. We know that the film is disordered when deposited at 300 K and annealing restores a LEED pattern. However, the LEED pattern is diffuse, possibly from a large population of defects. We also know from the depth profile of Fig. 8(a) that there appears to be some Ag on the surface of the film even before annealing. This migration of Ag at 300 K, in addition to the development of misfit dislocations in the film could be responsible for creating channels in the Rh layers through

which more Ag diffuses at higher temperatures. The population of these channel defects would then be expected to be larger for films grown at 600 K due to the continuous diffusion of Ag at this temperature. The XPS results which indicate a lower average atomic coordination for the Rh atoms for films grown at 600 K lend support to this statement. These results lead us to believe that diffusion of Ag (driven by the large difference in surface free energies) through defects created in the Rh film is the dominant mechanism which leads to the formation of the sandwich structure.

Comparison with other work. Ours is not the first evidence for surface enrichment of Ag in a Rh/Ag system. Anderson *et al.*⁴⁸ and Rouco *et al.*,⁴⁹ working with silica-supported, Rh-Ag particles, found evidence of Ag on the surface of Rh particles in a thin layer, perhaps only one atom thick. Their x-ray-diffraction results suggest the presence of separate Rh and Ag phases. These observations are similar to our own.

We have found only three other cases of “sandwich” structures in the literature. Chen *et al.*,⁵⁰ working with Ag on Pb(111), Rawlings *et al.*,⁵¹ working with Ag on Pb(111) and Cu on Pb(111), and Bader *et al.*,⁵² working with Fe on Au(100), all report results similar to our own. In all cases a monolayer of the substrate metal is found to be present at the surface after deposition of the overlayer material. These are metals which should be totally immiscible, or at least have very limited miscibilities, in the temperature range under consideration. Similar to the Rh/Ag system, the driving force in these cases is thought to be the large difference in surface free energies (the substrate being the much lower surface-free-energy material) and immiscibilities of the overlayer and substrate metals. These findings indicate that for metal-on-metal systems of this category sandwiches may be a general phenomenon and should be considered in addition to the three long-standing modes of equilibrium growth.

We believe that this phenomenon may not be restricted to these three systems. There are several instances where the growth mode of analogous systems is controversial.^{8,9,11,14} In these instances the substrate is often assumed to be a rigid, stationary template, with the structure of the overlayer depending only on overlayer atom mobility, electronic interactions, lattice mismatches, and surface-energy constraints. However, we have shown that substrate atom mobility can provide additional pathways to satisfying thermodynamic requirements.

CONCLUSIONS

We have found that the mode of growth of the Rh/Ag(100) system does not follow any of the three classical growth modes, (i.e., Frank–van der Merwe, Stranski-Krzanstov, or Volmer-Weber modes). In a system such as this where the free energy of the film is greater than that of the substrate, and the free energy of the interface is thought to be small, Volmer-Weber growth mode is expected. Traditionally it is thought that

the film will grow as three-dimensional crystallites to expose a large area of the substrate and thus keep the surface energy at a minimum. However, if the mobility of the substrate atoms is sufficient to allow diffusion which results in a lowering of the surface energy, agglomeration need not be invoked. We believe that this is the case for the Rh/Ag(100) system which leads to the formation of a Ag-Rh-Ag sandwich structure. The essential feature in this system is the substrate atom mobility. Growth in this manner may be typical for immiscible systems and those with limited solubility which also possess large differences in surface free energies, the extent of substrate diffusion being governed by the magnitude of these energy differences and solubilities.

ACKNOWLEDGMENTS

We thank R. J. Baird for the use of his vacuum system, in which the XPS, UPS, and ISS studies were completed, and T. Potter for technical assistance in using the equipment. We also thank A. J. Bevolo for making his SAM chamber available to us and for helping us to use it. This work was supported by a grant from the Ford Motor Company; and one of us (P.A.T.) is supported by the National Science Foundation (Grant No. CHE-84-51317) and by the Camille and Henry Dreyfus Foundation. In addition, some equipment and all facilities were provided by the Ames Laboratory, which is operated for the U.S. Department of Energy by Iowa State University under Contract No. W-7405-ENG-82.

*Present address: Ford Motor Company, Dearborn, MI 48121.

¹E. Bauer, *Appl. Surf. Sci.* **11/12**, 479 (1982).

²C. H. F. Peden and D. W. Goodman, *J. Catal.* **100**, 520 (1986).

³P. J. Berlowitz, J. E. Houston, M. M. White, and D. W. Goodman, *Surf. Sci.* **205**, 1 (1988).

⁴E. Bauer, *Z. Kristallogr.* **110**, 372 (1958).

⁵P. A. Dowben, M. Onellion, and Y. J. Kime, *Scanning Microscopy* **2**, 177 (1988).

⁶D. Prescia, M. Stampanoni, G. L. Bona, A. Vaterlaus, R. F. Willis, and F. Meier, *Phys. Rev. Lett.* **58**, 2126 (1987).

⁷W. Daum, C. Stuhlmann, and H. Ibach, *Phys. Rev. Lett.* **60**, 2741 (1988).

⁸D. A. Steigerwald and W. F. Egelhoff, Jr., *Phys. Rev. Lett.* **60**, 2558 (1988).

⁹D. Prescia, M. Stampanoni, G. L. Bona, A. Vaterlaus, F. Meier, G. Jennings, and R. F. Willis, *Phys. Rev. Lett.* **60**, 2559 (1988).

¹⁰D. A. Steigerwald and W. F. Egelhoff, Jr., *Surf. Sci.* **202**, 472 (1988).

¹¹S. A. Chambers, T. J. Wagner, and J. W. Weaver, *Phys. Rev. B* **36**, 8992 (1987).

¹²S. D. Bader, E. R. Moog, and P. Grünberg, *J. Magn. Magn. Mater.* **53**, L295 (1986).

¹³G. C. Smith, H. A. Padmore, and C. Norris, *Surf. Sci.* **119**, L287 (1982).

¹⁴J. W. A. Sachlter, M. A. Van Hove, J. P. Biberian, and G. A. Somorjai, *Surf. Sci.* **110**, 19 (1981); also E. G. Michel, M. C. Asensio, and S. Ferrer, *ibid.* **198**, L365 (1988).

¹⁵L. Z. Mezey and J. Giber, *Jpn. J. Appl. Phys.* **21**, 1569 (1982).

¹⁶B. C. DeCooman and R. W. Vook, *J. Vac. Sci. Technol. A* **21**, 899 (1982).

¹⁷G. E. Rhead, M. G. Barthes, and C. Argile, *Thin Solid Films* **82**, 201 (1981).

¹⁸T. E. Gallon, *Surf. Sci.* **17**, 486 (1969).

¹⁹G. E. Rhead, M.-G. Barthes, and C. Argile, *Thin Solid Films* **82**, 201 (1981).

²⁰E. Bauer, H. Poppa, G. Todd, and P. R. Davis, *J. Appl. Phys.* **48**, 3773 (1977).

²¹S. L. Beauvais, R. J. Behm, S.-L. Chang, T. S. King, C. G. Olson, P. R. Rape, and P. A. Thiel, *Surf. Sci.* **189/190**, 1069 (1987).

²²P. I. Cohen, G. S. Petrich, P. R. Pukite, G. J. Whaley, and A. S. Arrott, *Surf. Sci.* **216**, 222 (1989).

²³J. W. Evans, *Phys. Rev. B* **39**, 5655 (1989).

²⁴M. P. Seah and W. A. Dench, *Surf. Interface Anal.* **1**, 2 (1979).

²⁵A. G. Knapp, *Surf. Sci.* **34**, 289 (1973).

²⁶D. E. Peebles, H. C. Peebles, and J. M. White, *Surf. Sci.* **136**, 463 (1984).

²⁷G. C. Smith, C. Norris, C. Binns, and H. A. Padmore, *J. Phys. C* **15**, 6481 (1982).

²⁸D. K. Flynn, W. Wang, S.-L. Chang, M. C. Tringides, and P. A. Thiel, *Langmuir* **4**, 1096 (1988).

²⁹D. K. Flynn, J. W. Evans, and P. A. Thiel, *J. Vac. Sci. Technol. A* **7**, 2162 (1989).

³⁰J. W. Evans, D. K. Flynn, and P. A. Thiel, *Ultramicroscopy* (to be published).

³¹I. Karakaya and W. T. Thompson, *Bull. Alloy Phase Diagrams* **74**, 362 (1986).

³²W. Schlenk and E. Bauer, *Surf. Sci.* **93**, 9 (1980).

³³H. C. Peebles, D. D. Beck, J. M. White, and C. T. Campbell, *Surf. Sci.* **150**, 120 (1985).

³⁴Y. Kim, H. C. Peebles, and J. M. White, *Surf. Sci.* **114**, 363 (1982).

³⁵R. A. Marbrow and R. M. Lambert, *Surf. Sci.* **67**, 489 (1977).

³⁶D. G. Castner, B. A. Sexton, and G. A. Somorjai, *Surf. Sci.* **71**, 519 (1978).

³⁷K. Kawasaki, M. Shibata, H. Miki, and T. Kioka, *Surf. Sci.* **81**, 370 (1979).

³⁸P. H. Citrin, G. K. Wertheim, and Y. Baer, *Phys. Rev. B* **27**, 3160 (1983).

³⁹G. W. Graham, *Surf. Sci.* **171**, L432 (1986).

⁴⁰S. H. Lu, Z. Q. Wang, S. C. Wu, C. K. C. Lok, J. Quinn, Y. S. Li, D. Tian, and F. Jona, *Phys. Rev. B* **37**, 4296 (1988).

⁴¹S. C. Wu, S. H. Lu, Z. Q. Wang, C. K. C. Lok, J. Quinn, Y. S. Li, D. Tian, and F. Jona, *Phys. Rev. B* **38**, 5363 (1988).

⁴²G. W. Graham, *Surf. Sci.* **184**, 137 (1987).

⁴³C. Koziol, G. Lilienkamp, and E. Bauer, *Appl. Phys. Lett.* **51**, 901 (1987).

⁴⁴M. Jaxochaswski and E. Bauer, *J. Appl. Phys.* **63**, 4501 (1988).

⁴⁵W. F. Egelhoff, Jr. and I. Jacob, *Phys. Rev. Lett.* **62**, 921, 1577(E) (1989).

⁴⁶S. Mukherjee and J. L. Moran-Lopez, *Surf. Sci.* **188**, L742 (1987).

⁴⁷P. M. Ossi, *Surf. Sci.* **201**, L519 (1988).

⁴⁸J. H. Anderson, P. J. Conn, and S. G. Brandenberger, *J. Catal.* **16**, 404 (1970).

⁴⁹A. J. Rouco and G. L. Haller, *J. Catal.* **72**, 246 (1981).

⁵⁰C. H. Chen and F. J. Sansalone, *Surf. Sci.* **164**, L688 (1985).

⁵¹K. J. Rawlings and P. J. Dobson, *Thin Solid Films* **67**, 171 (1980).

⁵²S. D. Bader and E. R. Moog, *J. Appl. Phys.* **61**, 3729 (1987).

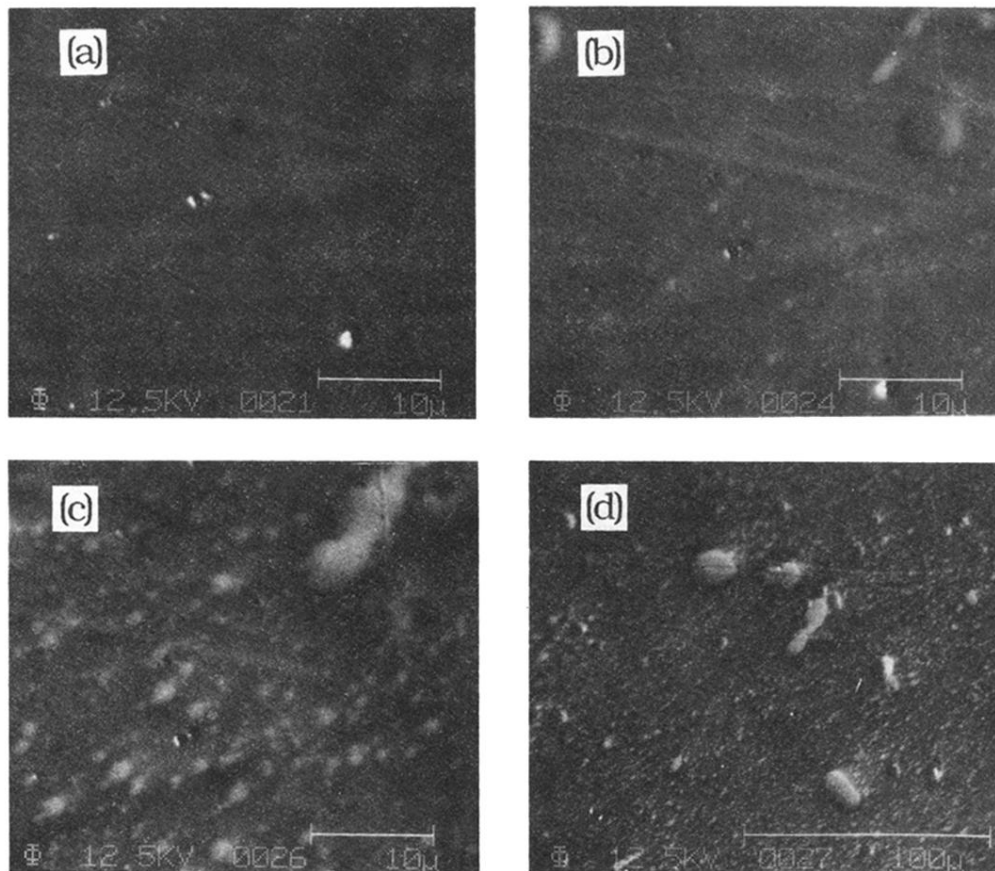


FIG. 11. Electron micrographs of a thick, ≈ 16 -layer Rh film. Sample temperature is held at 380 K. (a) Carbon- and sulfur-contaminated surface (2510 \times). (b) As in (a), ion-etched to remove the carbon and sulfur, 60 sec after turning off the ion beam (2510 \times). (c) As in (b), 15 min after turning off ion beam (2510 \times). (d) As in (c), magnification of 508 \times .